Published by
NIGERIAN SOCIETY OF PHYSICAL SCIENCES
Available online @ https://journal.nsps.org.ng/index.php/jnsps

J. Nig. Soc. Phys. Sci. 5 (2023) 1248

Journal of the Nigerian Society of Physical Sciences

Bivariate and Partial Wavelet Coherence analysis of aerosols impact on Global Horizontal Irradiation in Far-North and Littoral regions of Cameroon

Douanla Alotse Yaulande[a,*], Mamadou Ossénatou[a], Dembélé André[b], Lenouo André[c]

[a] *Physics, Institute of Mathematics and Physics (IMSP), Dangbo, Bénin*
[b] *Operations Research and Optimization, Department of Mathematics and Informatics, Faculty of Sciences and Technics (FST), Mali*
[c] *Laboratory of Physics, University of Douala, Cameroon*

Abstract

This study investigated the time-frequency variability of Global Horizontal Irradiation (GHI) under clear sky conditions in Cameroon in relation to aerosol types using the wavelet transform method. For this purpose, we focused on two climatically different zones (Far North and Littoral) in Cameroon chosen because of the large difference in term of proportion in type of aerosols. From the Bivariate Wavelet Coherence (BWC) analysis, it was found in the Littoral zone (Dust DU, Organic Matter OM, Black Carbon BC, Sulfates SU) aerosols are negatively correlated with GHI at all frequencies, whereas Sea Salt (SS) aerosols are positively correlated with GHI. In the Far North zone, all aerosols are negatively correlated with GHI in the 0-8 month band but the dynamic has changed in the 8-16 month band. However, with the Partial Wavelet Coherence (PWC) analysis, we found that the correlations between GHI and each analyzed variable decreased after removing the effects of the remaining variables. Only the correlations between GHI and DU are still significant, with an average wavelet coherence (AWC) and percentage of significant coherence (PASC) values of 0.60 and 24.36% respectively. It is noteworthy with PWC analysis that the area with significant correlation between GHI and the other aerosol types except DU is very limited. This shows that their influences on GHI have already been covered by DU. The study also showed the combined effect of the analyzing variables (SS, BC, SU and OM) on GHI, since, independently as shown by the PWC, each of them is weakly correlated to GHI. However, with the BWC, the combined effect of other aerosols on BC and SU makes their influences on GHI important. The PWC and BWC implementations have been compiled by Matlab and can be accessed freely following this link (https ://figshare.com/s/bc97956f43fe5734c784).

DOI:10.46481/jnsps.2023.1248

Keywords: Irradiation, Biwavelet, Partial wavelet coherence, Aerosols, Cameroon

Article History :
Received: 29 November 2022
Received in revised form: 11 January 2023
Accepted for publication: 14 January 2023
Published: 27 February 2023

Communicated by: B. J. Falaye

1. Introduction

Renewable energies have been drawing increasing attention in recent decades [1, 2]. They are at the heart of many scientific debates and are therefore intensively encouraged by governments in many countries [3, 4]. Indeed, renewable energy

*Corresponding author tel. no: +229 62206100
Email address: yaulande.douanla@imsp-uac.org (Douanla Alotse Yaulande)

is among the top choices solutions regarding both the reduction of carbon dioxide emissions, and the limitation of local air pollution of carbonaceous aerosols from both fossil combustion and other anthropogenic activities [5, 6]. Solar energy, in this context, is one of the most important renewable energies as it is clean, abundant and available worldwide. Moreover, it is indirectly the basis of all other renewable energies (wind, geothermal, etc.). It offers a wide range of uses, such as for energy production (electricity, heating) for households and even for commercial purposes and so forth. For this purpose, the study of the availability of solar energy and factors inducing its surface variability is relevant for determining the appropriate strategic areas for sustainable energy exploitation [7–9].

For example, for photovoltaic (PV) energy production in a given location, the assessment of the availability of Global Horizontal Irradiation (GHI) and factors inducing its fluctuation are an important step because the efficiency of photovoltaic energy production is influenced by several factors including atmospheric parameters varying according to the location. The amount of available energy also highly depends on the sky conditions (clear or cloudy) [9–11]. In clear sky conditions, incident rays are mostly attenuated by atmospheric aerosols [12], which refers to fine solid or liquid particles suspended in the atmosphere. These particles are of various types and are spatially unevenly distributed. Several studies have shown the dependence of the amount of solar energy available at a location on aerosol types and quantity [13–16]. In Cameroon, a machine learning model is built to predict the Direct Normal Irradiation (DNI) as a function of the different aerosol types and by Shapley's explanatory method we show that DNI is mostly influenced by desert dust aerosols following by organic carbon aerosols, [17]. The authors also studied in [18] the temporal and frequency variability of the DNI in 9 different climatic zones across Cameroon as a function of aerosol types. Based on a wavelet analysis, it is shown that the frequency of variability and the intensity of the correlation between the DNI and aerosols varies according to the aerosol types and zones. However, at all frequencies the existing correlation is negative.

Knowing that the Global Horizontal Irradiation (GHI) is the sum of the direct normal and diffuse energies, it is important to know whether the order of an aerosol's impact on GHI is the same as on DNI and also if the correlation frequencies are the same in both cases. The objective of this study is therefore to analyze the time-frequency relationship between Global Horizontal Irradiation (GHI) and Desert Dust aerosols (DU), Black Carbon (BC), Organic Carbon (OC), Sea Salt (SS) and Sulphate (SU) in two climatically different areas of Cameroon (Far North and Littoral). Given that for a two-dimensional analysis (time-frequency), the wavelet analysis method is the most suitable [19–21], the analysis is undertaken using bivariate coherence (BWC) and partial wavelet coherence (PWC) methods. In the rest of the paper, we present the used data, describe the different methodological approaches, and then highlight the findings, following by a conclusion.

2. Data and method

2.1. Data

The study area (Cameroon see Fig 1) is a Central African country which gathers in its 475 442 km^2 the essential of what is offered elsewhere in Africa : hence the appellation Africa in miniature [22, 23].

The study is based on a monthly data set collected from January 2005 to December 2019 (181 observations) of 2 different climatic zones located in the Littoral and Far North regions of Cameroon (see Fig 1). Monthly series of global horizontal irradiation under clear skies (GHI) are obtained from hourly data provided by the Copernicus Atmosphere Monitoring Service (CAMS) radiation service (http://www.soda-pro.com/web-services/radiation/cams-radiation-service) with a spatial resolution of 0.58°x0.6258°. Monthly aerosol optical depth series of different aerosol types (Sea Salts (SS), black carbon (BC), Organic Carbon (OM), Desert Dust (DU) and Sulfate aerosols (SU)) are obtained from hourly data provided by CAMS-AOD (http://www.soda-pro.com/web-services/atmosphere/cams-aod).

2.2. Biwavelet coherence (BWC) and phase function

In order to identify the degree of correlation between two signals, wavelet coherence and phase coherence analysis techniques are often used. In fact, the wavelet coherence formulation (Eq. 1) displays the correlation of two signals at different frequencies s (or scales) relative to time t [24, 25]. It ranges between 0 and 1.

$$C_{xy}(s,t) = \frac{|S\, s^{-1} W_{xy}(s,t)|}{\sqrt{S(s^{-1} j W_x(s,t) j^2) S(s^{-1} j W_y(s,t) j^2)}}, \qquad (1)$$

with

$$W_{xy}(s,t) = W_x(s,t) W_y^*(s,t). \qquad (2)$$

$S = S_s\Big(S_t(W_{xy}(s,t))\Big)$ is the smoothing factor [26]. In Eqs. (1 and 2), $W_x(s,t)$ expressed as follows is the continuous Wavelet Transform (CWT) of a given signal.

$$W_x(s,t) = \int_{-\infty}^{+\infty} x(\tau) \Psi_{s,t}^*(\tau) d\tau, \qquad (3)$$

where $\Psi_{s,t}^*(\tau)$ is the conjugate of $\Psi_{s,t}(\tau)$ ([26]).

The phases $\theta_{xy}(s,t)$ (Eq. 4) are obtained based on the imaginary and real parts of the cross spectrum $W_{xy}(s,t)$.

$$\theta_{xy}(s,t) = \tan^{-1}\Big(\frac{Im(W_{xy}(s,t))}{Re(W_{xy}(s,t))}\Big), \qquad (4)$$

with $\theta_{xy} \in [-\pi, +\pi]$ in radians.

2.3. Partial wavelet coherence (PWC)

Similar to wavelet coherence, Partial Wavelet Coherence (PWC) allows to identify the correlation between two time series. With the PWC, one can investigate the correlation between two data sets while excluding the influence of their common dependence [27]. In order to exclude more than one variable (for

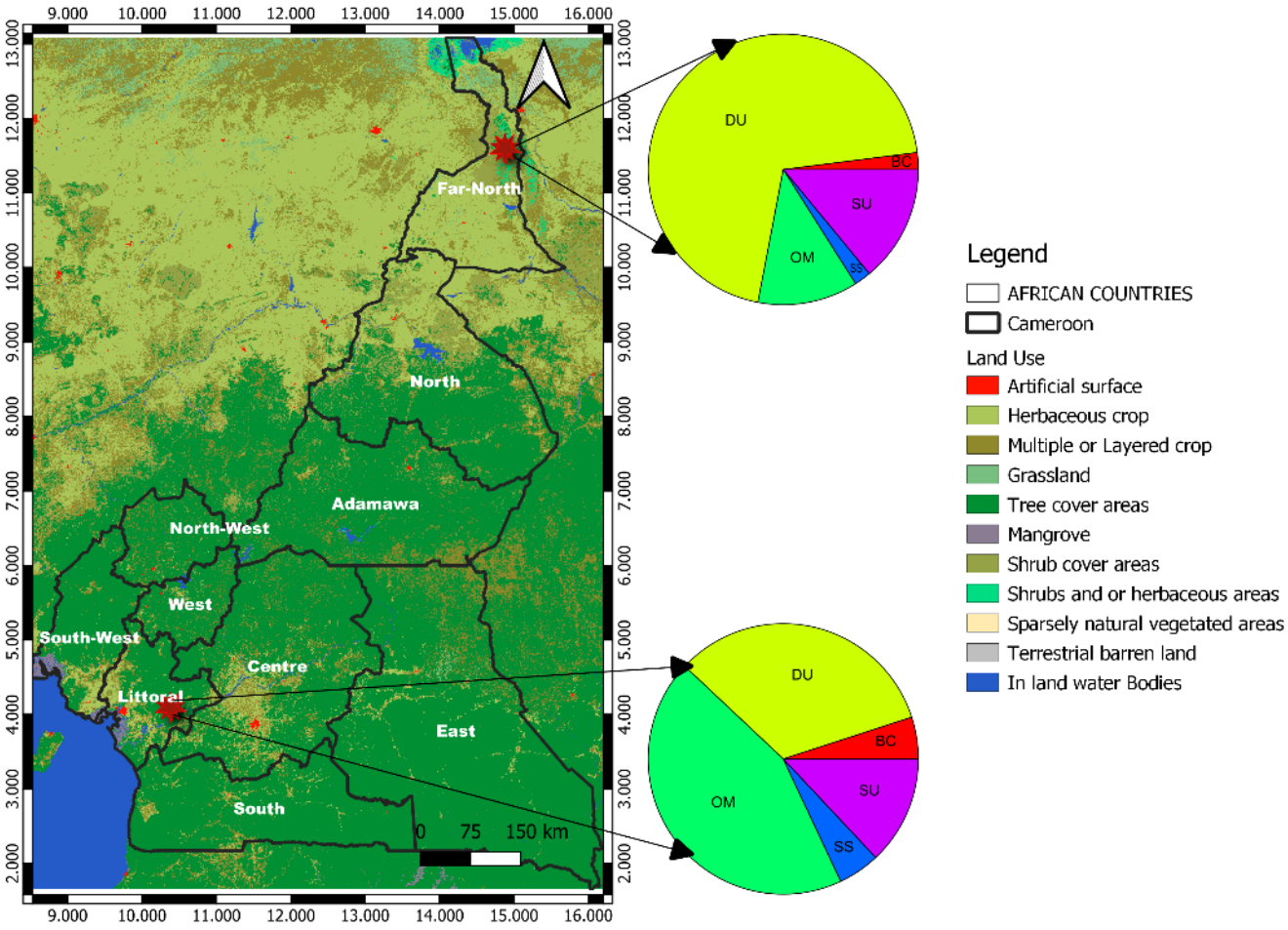

Figure 1: Land Use Map of study area using OpenStreetMap data (http://download.geofabrik.de/africa/cameroon-latest-free.shp.zip). The red stars represent the position of selected study areas. According to [18] the selected zones are among the 9 zones strategically selected by the K-means method. The pie charts provide information on the average percentage of aerosol types in the studied areas.This statistical representation by the pie chart shows that, on average, in the Northern zone, Desert Dust aerosols (DU) dominate at almost 75% followed almost proportionally by Sulfate aerosols (SU) and Organic Carbon (OM). However, in the Littoral zone, OM dominates, followed by DU and SU.

example, to calculate the PWC of $X1$ on Y by controlling the effects of $X2$, $X3$, $X4$, $X5$ as in our case study) PWC is expressed as follows [28]:

$$P^2_{ij|(\backslash ij)}(s,t) = \frac{|m^{ij}(s)|^2}{|m^{ii}(s)|^2|m^{jj}(s)|^2}, \tag{5}$$

where $P^2_{ij|(\backslash ij)}$ is the partial wavelet coherence squared between $x_i(t)$ and $x_j(t)$ when controlling other variables. m^{ij} is the `(i,j)` element of the inverse spectral matrix $m^{-1}(s)$ ($m(s)$ expressed below in which $W(s,t)$ is the CWT of each time serie [26, 29]), $(\backslash ij)$ signifies all elements excluding the i^{th} and the j^{th}.

$$m(s) = \begin{vmatrix} W_{11}(s,t) & W_{12}(s,t) & \dots & W_{1n}(s,t) \\ W_{21}(s,t) & W_{22}(s,t) & \dots & W_{2n}(s,t) \\ . & . & \dots & . \\ . & . & \dots & . \\ . & . & \dots & . \\ W_{n1}(s,t) & W_{n2}(s,t) & \dots & W_{nn}(s,t) \end{vmatrix}$$

2.4. Significance of correlation

As an alternative way to statistically evaluate the correlation between two variables, the average wavelet coherence (AWC) and the percent significant coherence (PASC) can be calculated [30].

AWC is the average value of wavelet coherence occurring across all scales and PASC is the percentage of significant values among the total number of power values resulting from the

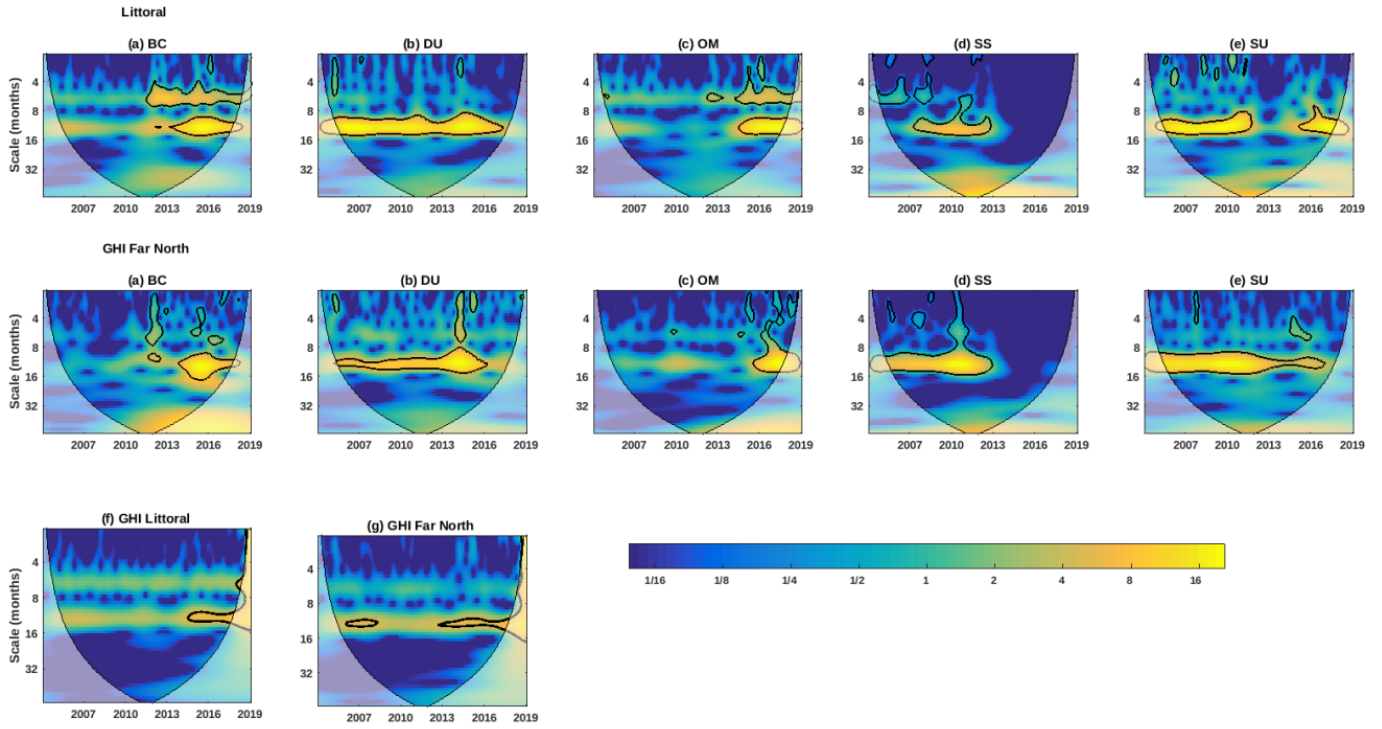

Figure 2: Continuous wavelets of monthly aerosols types : Littoral's zone a, Far North's zone at the middle and GHI. Black contours denote 5% significant levels against red noise. The U-shaped curve is the cone of influence that limits the edge effects that can distort the results.

BWC or PWC calculation. Significant power is the one with the ratio of the wavelet coherence power to the significance level greater than 1. Therefore, high values of AWC and PASC denote the prevalence of significant correlation areas between the two variables involved.

3. Results and Discussion

3.1. Continuous Wavelet Transform analysis (CWT) of GHI and aerosols types

In [18] from the intra-annual variability study of aerosol types, it is found that in the Far North zone, dust aerosols (DU) are the most abundant aeorosol relatively to the other types throughout the year although and its maximum amount is reached in March. Whereas in the Littoral, dust aerosols (DU) and organic carbon (OM) aerosols are almost equal and also follow the same seasonal variation throughout the year. Thus, in this area, the OM reaches its maximum in December while the DU reaches its maximum in March.

The CWT spectra $|W_x(s,t)|^2$ of the different studied variables in the Northern and Coastal areas are presented in (Fig 2) where the first line of the panel displays the results for the Littoral and the Far North respectively. Time-frequency localized variations in the aerosols types and GHI time series are obtained using Morlet mother wavelet [29]. In (Fig 2), black contours enclose the areas where the spectral power is 95% significant [24].

The wavelet transform analysis reveals an important periodic fluctuation in the 8-16 months band although it is very low for all aerosol time series in both studied areas, except for OM and BC, for which fluctuations appear after 2013. However, during the same year, the fluctuations become insignificant in both areas for SS (Sea Salt) (Fig 2 d). Regarding the temporal localization in both zones, DU is the most localized in the 8-16 month band across all years analyzed, while this trend or feature appears only in the Far North for the SU particles (Fig 2 e).

Table 1: average wavelet coherence (AWC) and the percentage of the significant power at a 95% significance level (PASC)

	Littoral		Far North	
	AWC	**PASC** (%)	AWC	**PASC** (%)
GHI & BC	0.636	**49.67**	0.45	**23.44**
GHI & DU	0.52	**29.96**	0.52	**29.94**
GHI & OM	0.638	**46.60**	0.49	**31.08**
GHI & SS	0.42	**22.49**	0.51	**21.97**
GHI & SU	0.43	**22.29**	0.50	**25.43**

3.2. Coherence analysis

Fig 4 displays the relationships between the five aerosol types and GHI for the littoral (a) and Far North (b) zones. The phase relationships between the time series are indicated in the figure with arrows [24]. As expected, the BWC results obtained differ according to variables and areas.

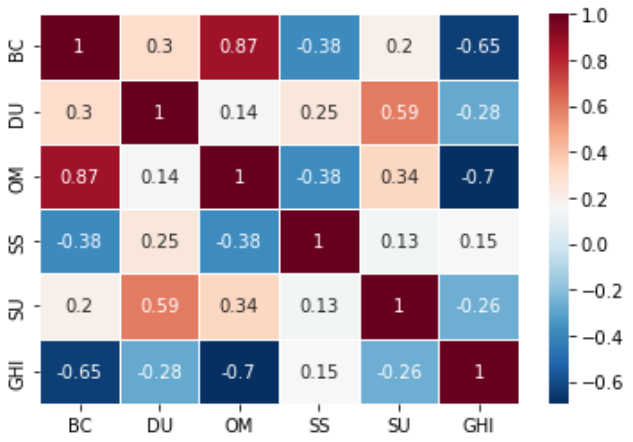

(a) Littoral

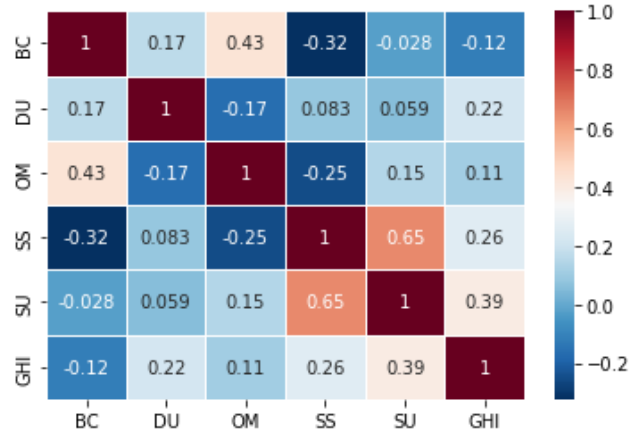

(b) Far North

Figure 3: Pearson correlation's map between the monthly average of GHI and aerosols types for the littoral (a) and Far North (b) zones in the studied period (2005-2019).

In the littoral zone (Fig 4 a), the correlations are mainly between a 4-16 month band for BC and OM and SS (although the correlation with SS is not as important as for BC and OM because, after 2013, the correlation is no longer significant) and mainly between 8 to 16 months for DU and SU. Regarding their phase relationships, in the Littoral (Fig 4 a), in the significantly correlated bands, all aerosols, except SS, are inversely correlated with GHI, since the arrows point to the left. Moreover, the peaks are oriented upwards, highlighting a phase advance of the aerosols over GHI. In that area, the AWC and PASC are respectively (0.636 and 46.67%) between GHI and BC, (0.52 and 29.96%) for GHI and DU, (0.638 and 46.60%) for GHI and OM, (0.42 and 22.49%) for GHI and SS and (0.43 and 22.49%) for GHI and SU. So the most correlated aerosols to GHI are BC and OM with at almost equal AWC and PASC values (see Tab 1). In the northern area (Fig 4 b), the correlation bands are almost similar to those observed in the littoral area, although with the exception of BC, which is anti-correlated to DNI, all the remaining aerosol types at frequency (<8 month) are anti-correlated to DNI (arrows pointing left) and at frequency (>8 month) are positively correlated (arrows pointing right). Moreover, the correlation intensity decreases in some cases, like between GHI, BC and OM, and increases in the case of GHI, SS and SU and for GHI and DU, the correlation remained the same as in the Littoral area (see AWC and PASC values in Tab 1). One can retain that among the five aerosol species, the most correlated aerosols to GHI in the Northern area is DU (see Tab 1). Also, this particle has been found as the most influencing variable since a negative relationship with GHI was obtained at two different frequencies (0-4 month band and 6 months) during the study period.

3.3. Partial Wavelet Coherence analysis

The BWC investigation between each analyzing variable and the Global Horizontal Irradiation (GHI) previously studied is done without dissociating the existing correlations between the analyzing variables. Knowing that the correlation between variables can be influenced by their relationship with the other remaining variable, the PWC analysis allows to better appreciate each connection by eliminating each time the influence of other analyzing variables on the one whose correlation with GHI is searched according to [30, 31] approach.

Regardless of the zones, the PWC analysis gives different information than those obtained earlier with BWC. Indeed, after excluding the effect of the other four aerosol types on the aerosol type whose correlation with GHI is sought, the results are in all cases quite different; correlation is very weak compared to the previous case (see Tab 2 for PWC compared to Tab 1 for BWC) and the areas of significant correlations are sparse.

In general, excluding the effect of other variables with the partial wavelet analysis, only DU influences the GHI in both the areas AWC and PSC (Tab 2 and Tab 1). However, since the atmosphere is a chaotic system, aerosols interact with each other as shown in the Pearson matrix (Fig 3) and may induce a combined effect on the GHI. The correlation matrix of each zone identifies the correlation degree of aerosols types together and between aerosols and the GHI.

From the Pearson correlation map (Fig 3) and BWC analysis, we noticed that in the littoral zone, the SS is positively correlated to the GHI, whereas in the Far North, for frequencies lower than 6 months, apart from the BC, all aerosol types are positively correlated to GHI and inversely, for frequencies higher than 6 months. In order to understand the reason behind such a transition, we repeated the analysis for a single year (2014) in order to look for intra-annual phenomena that could cause such a phase change. Results are presented in Fig 6. In Fig (4 a), GHI-SS is negatively correlated at high frequencies and positively correlated at low frequencies. However, in Fig (6 a), at frequencies < 16 days they are negatively correlated but, in May the correlation is positive, which may explain the positive correlation obtained on the annual scale in Fig (4 b). As for Fig (6 b), for all aerosol types and at all frequencies the correlation is negative between each type and GHI. This implies that the positive correlation obtained on the annual scale on Fig (4 b) is related to a phenomenon that occurs once a year

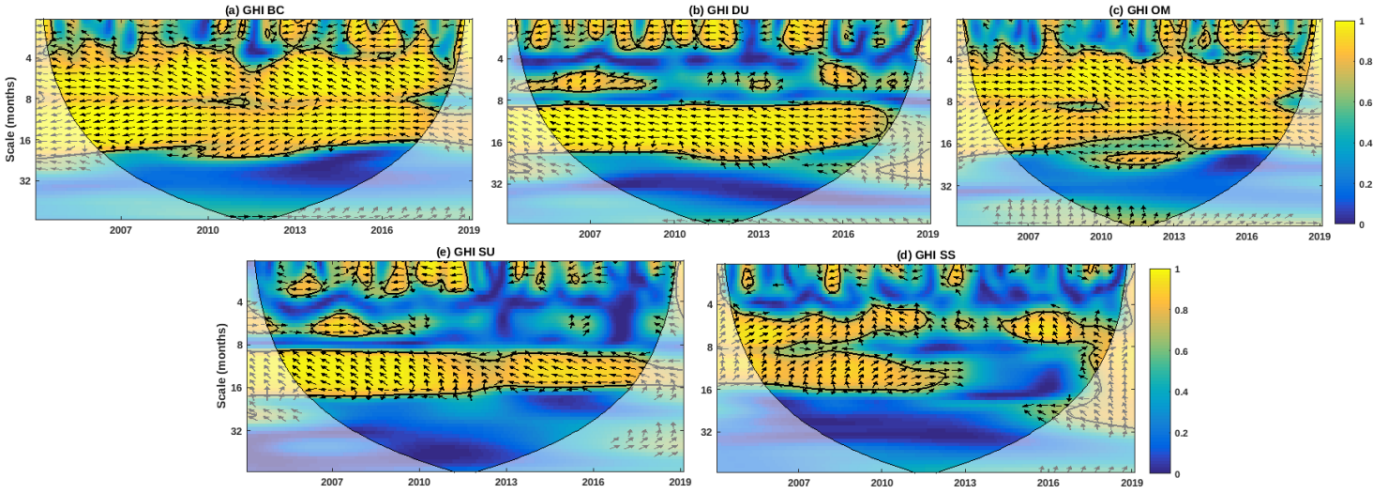

(a) Littoral

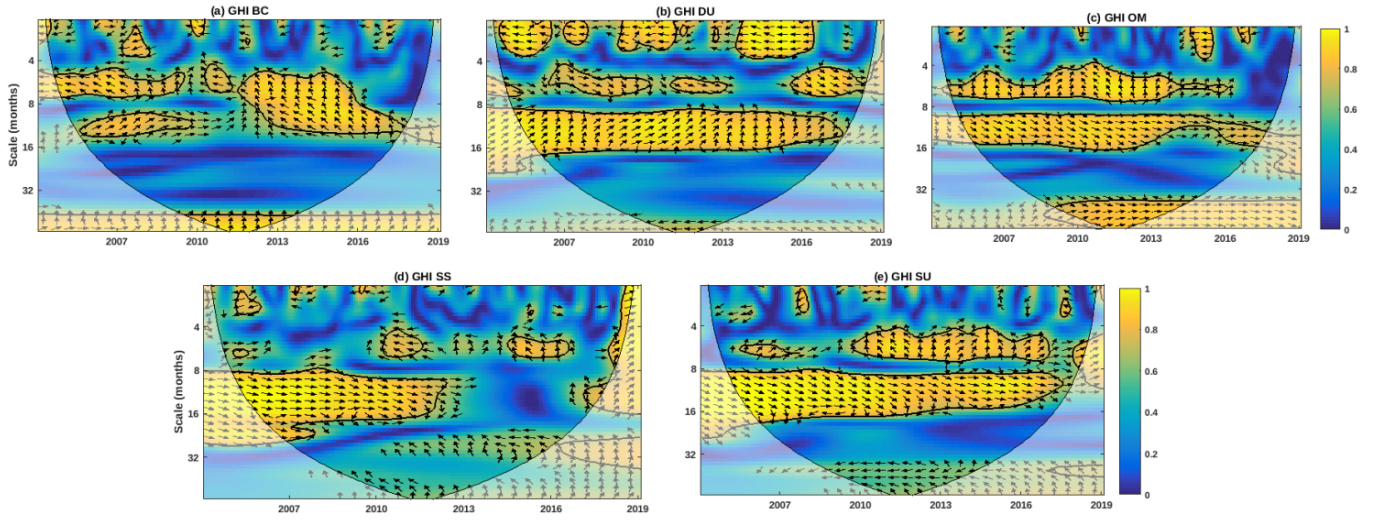

(b) Far North

Figure 4: Monthly bivariate wavelet transform coherence between GHI series and aerosols types : Littoral's zone (a) and Far North's zone (b). Each subplot shows the wavelet transform coherence between GHI in a single zone and the individual aerosol type that best explains GHI variation in that zone. Black contours denote 5% significant levels of red noise. The U-shaped curve is the cone of influence that limits the edge effects that can distort the results. Arrows denote the phase relationship (out of phase, arrows point to the left and in phase otherwise). The colored legend indicates the level of consistency.

Table 2: Average wavelet coherence (AWC) and the percentage of the significant power (PASC) values for partial wavelet coherence (excluding aerosols are in brackets).

	Littoral		Far North	
	AWC	PASC (%)	AWC	PASC (%)
GHI & BC (DU, OM, SS, SU)	0.44	10.01	0.47	9.82
GHI & DU (BC, OM, SS, SU)	0.60	24.36	0.57	19.34
GHI & OM (DU, BC, SS, SU)	0.54	13.31	0.50	15.26
GHI & SS (DU, BC, OM, SU)	0.51	16.74	0.55	21.44
GHI & SU (DU, BC, OM, SS)	0.44	7.98	0.54	18.83

in this area and it can not be attributed to the aerosol-energy relationship. In fact, the decrease in the amount of solar energy

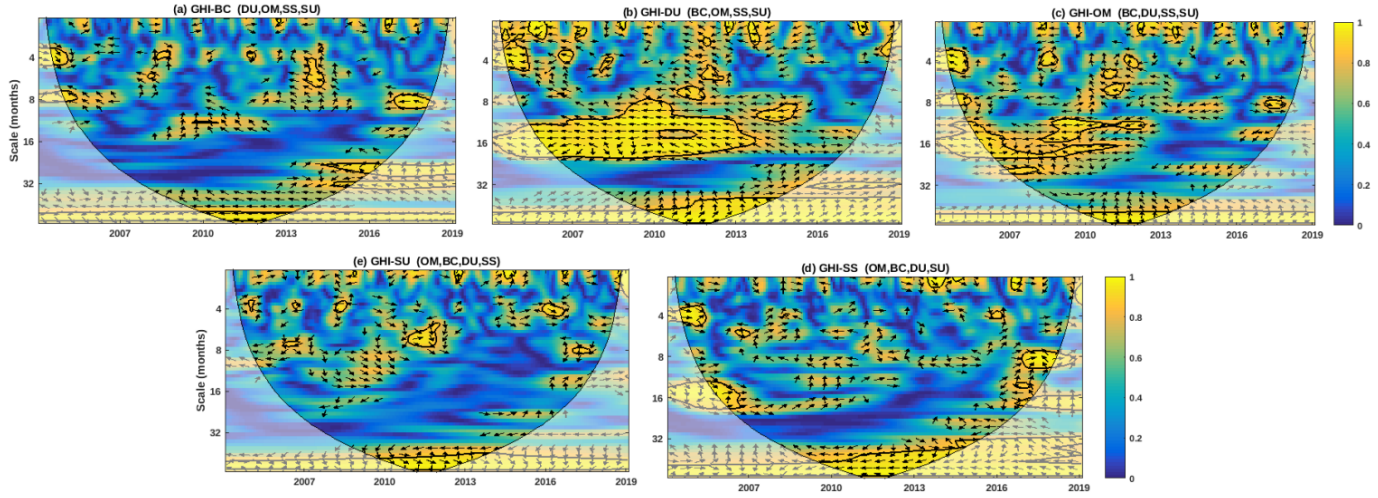

(a) Littoral

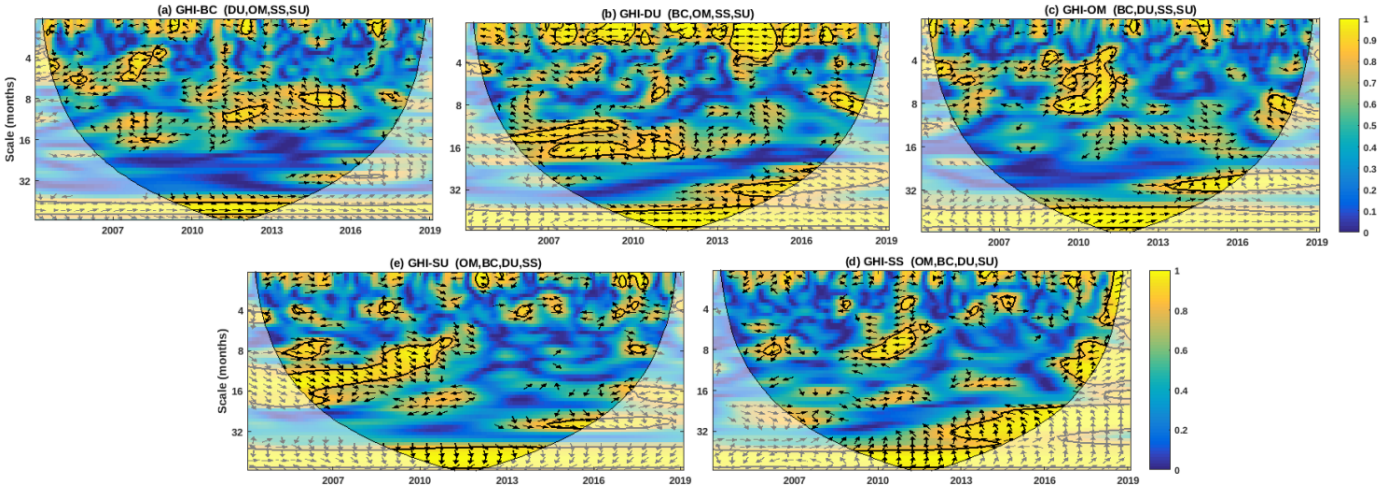

(b) Far North

Figure 5: Monthly Partial wavelet transform coherence between GHI series and aerosol types : Littoral's zone a and Far North's zone. Each subplot shows the wavelet transform coherence between GHI in a single zone and the individual aerosol type that best explains GHI variation in that zone. Black contours denote 5% significant levels of red noise. The U-shaped curve is the cone of influence that limits the edge effects that can distort the results. Arrows denote the phase relationship (out of phase, arrows point to the left and in phase otherwise). The colored legend indicates the level of consistency. Each card is titled as follows: GHI-(analyzed aerosols) (excluding aerosols).

is related to the rainfall that occurs once a year in the extreme north of Cameroon [32]. During that season, the amount of aerosols also decreases due to atmospheric leaching. So the positive correlation noted between aerosols and GHI between 8-16 months claiming that the decrease or increase of one of the variables should have the same effect on the other, is not the right explanation here, but rather the consequence of precipitation that reduces the sunshine duration and, at the same time, the atmospheric aerosol rate.

According to Fig (6 a), there is a strong correlation between GHI, BC, OM and SU from July to September, which corresponds to the periods when the optical thickness of BC, OM and SU reach their maximum because it is one of the harvesting seasons in the study area. The peak of OM, BC and SU during this period mainly comes from biomass and domestic burning. In addition, the same period corresponds to the vacation period, thus accentuating the release of BC and SU emissions from heavy traffic [33–35]. On the other hand, the correlation between GHI and DU is high between February and May, corresponding to the last quarter of the dry season which lasts from December to May in Cameroon [36]. However, in the Far North particularly, DU is correlated with GHI throughout the year (see Fig 6 b).

One of the key research questions of this study was to find out

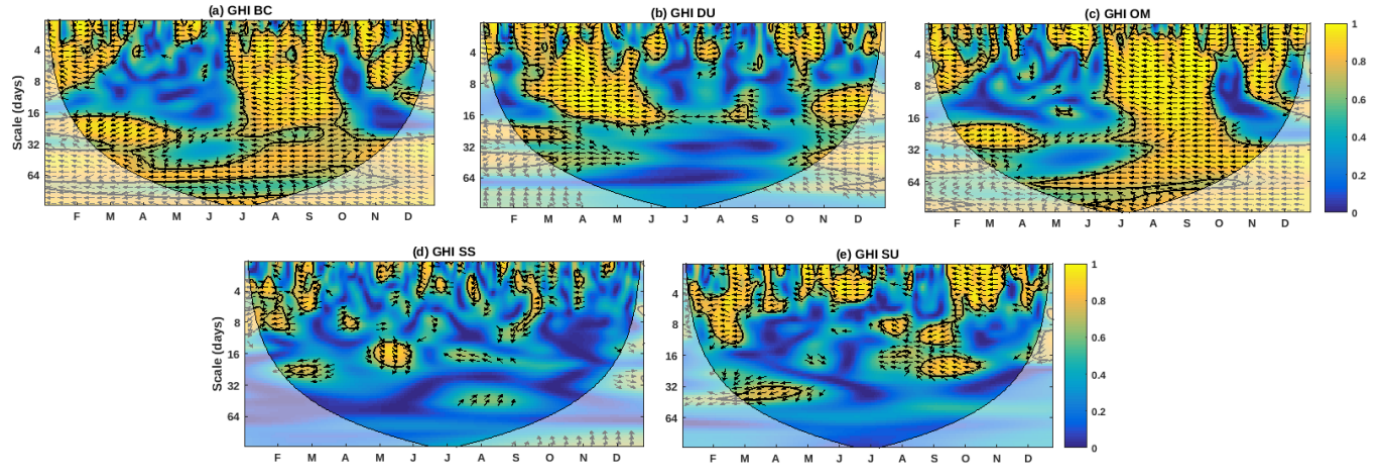

(a) Littoral

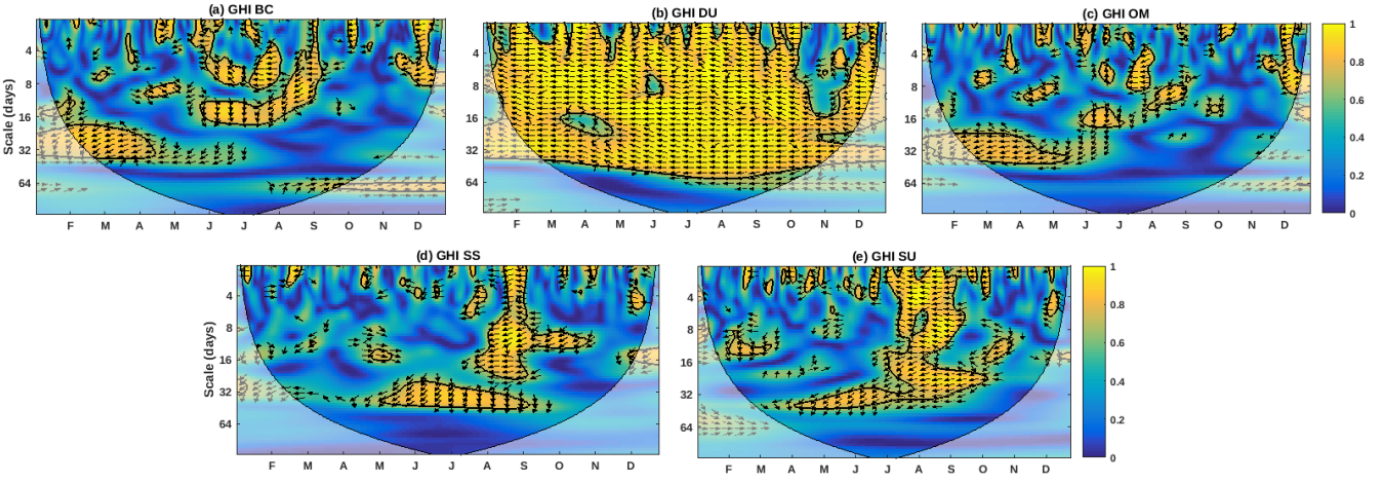

(b) Far North

Figure 6: Wavelet coherence (BWC) between daily average of GHI and aerosols time series (2014) : Littoral's zone a and Far North's zone.

whether, in these fields, aerosols were correlated at the same frequency with direct normal irradiation (DNI) [18] as with global horizontal irradiation (GHI) in clear sky conditions. We answer affirmatively to this question. However, at all frequencies, the aerosols are negatively correlated with the DNI, which is not the case with GHI. Moreover, the degree of correlation in the two cases is different, because the values of AWC and PASC are higher in the case of DNI than with GHI. This conclusion about the degree of correlation is predictable because the GHI, which is the sum of the direct and diffuse radiation, may not be too sensitive to the interface between the radiation particle because the radiation not collected in the direct component is collected in the diffuse component.

4. Conclusion

The Global Horizontal Irradiation (GHI), which is the main variable for solar photovoltaic energy modeling, was the subject of the present study. The study focused on two different climatological areas in Cameroon : Northern and Littoral regions based on wavelet analysis approaches to find the specific variability scales of each of the studied variables (GHI, BC, DU, OM, SS and SU). After that, the bivariate and partial wavelet coherence analysis was used to assess the nature and degree of correlation between each type of aerosol and GHI. The CWT analysis deployed on each of the time series revealed an annual periodicity for all variables, except for OM and BC, for which no periodicity was observed. As for the bivariate analysis, a strong correlation was observed between GHI and all aerosol types in the Littoral zone more than in the Far North because the AWC and PASC values are larger in that first zone (Littoral) than in the second. Additionally, in the Littoral, the most negatively correlated and therefore most attenuating aerosol types are OM and BC, whereas in the Far North, the most influenced is DU. Moreover, in the northern area at seasonal frequencies, all aerosols and GHI are negatively correlated (0-4 and 6 month

band) and, an annual frequency, apart from the BC, all other aerosols are positively correlated to the GHI. This positive correlation was associated with the rainy season that occurs once a year in this part of the country, which on that occasion decreases the sunshine duration as well as the atmospheric aerosol rate by leaching. Following the partial analysis, only DU isolated from any correlation with other aerosol types can significantly influence GHI. BC, This study provides important knowledge for future work and projects because, it gives information on the dynamics of aerosol fluctuations in the studied areas while considering its cyclical aspect, and explains the impact of such dynamics on GHI dynamics. Furthermore, this information can help to improve GHI prediction models, and also to explain the impact of some activities on the environment and the climate in general, since aerosols are partly coming from human activities.

Acknowledgements

This research was funded by the *German Academic Exchange Service* (DAAD) section ST32, (Grant No 57424259). The first author thanks IUPAP (International Union of Pure and Applied Physics) Women in Physics Travel Grant Program for financial support. Authors also thank Cams-AOD and CAMS-Radiation database administrators for providing open access to their databases.
The software for the multiple wavelet coherence and partial wavelet coherency was provided by W. Hu and B. C. Si, and is available from https://figshare.com/s/bc97956f43fe5734c784.

References

[1] M. Okono, E. Agbo, B. Ekah, U. Ekah, E. Ettah & C. Edet, "Statistical analysis and distribution of global solar radiation and temperature over southern Nigeria", Journal of the Nigerian Society of Physical Sciences **4** (2022) 588.

[2] A. S. Khalil, "Performance Evaluation and Statistical Analysis of Solar Energy Modeling: A Review and Case Study", Journal of the Nigerian Society of Physical Sciences, **4** (2022) 911.

[3] M. Matt & R. Babcock, "Renewable Energy Debate", CQ Researcher, https://us.corwin.com/sites/default/files/upm-assets/114665_book_item_114665.pdf, (2019).

[4] H. Sybille, N. Kai & A. Simone, "Renewable energy resources: how can science education foster an appropriate understanding?", European Science Education Research Association (2018).

[5] O. P. Asantewaa & A. Samuel, "A review of renewable energy sources, sustainability issues and climate change mitigation", Cogent Engineering **3** (2016) 1167990.

[6] G. Dolf, B. Francisco, S. Deger, B. Morgan, W. Nicholas & G. Ricardo, "The role of renewable energy in the global energy transformation", Energy Strategy Reviews, **24** (2019) 38.

[7] D. U. Chandra, K. G. Panagiotis, N. S. Shantikumar & M. Akriti, "Impact of aerosol and cloud on the solar energy potential over the central gangetic himalayan region", Remote Sensing **13** (2021) 3248.

[8] D. Yang, J. Panida & W. Wilfred M, "The estimation of clear sky global horizontal irradiance at the equator", Energy Procedia **25** (2012) 141.

[9] E. A. Omaima, G. Hicham, G. Abdellatif & D. Fatima-ezzahra, "Detection of clear sky instants from high frequencies pyranometric measurements of global horizontal irradiance", E3S Web of Conferences **229** (2021) 01008.

[10] Z. Guang & M. Yingying, "Clear-Sky Surface Solar Radiation and the Radiative Effect of Aerosol and Water Vapor Based on Simulations and Satellite Observations over Northern China", Remote Sensing **12**, (2020) 1931.

[11] Z. Evans, "Predicting clear-sky global horizontal irradiance at eight locations in South Africa using four models", Journal of Energy in Southern Africa **28** (2017) 77.

[12] F. Ilias *et al.*, "Effects of aerosols and clouds on the levels of surface solar radiation and solar energy in Cyprus", Remote Sensing **13** (2021) 2319.

[13] X. Weipeng, Z. Guangyuan & P. Stefan, "Estimation of global horizontal irradiance in China using a deep learning method", International Journal of Remote Sensing **42** (2021) 3899.

[14] G. Emily, T. Velle, N. K. Pagh, R.Laura & M. Ján, "Effects of aerosols on clear-sky solar radiation in the ALADIN-HIRLAM NWP system", Atmospheric Chemistry and Physics **16** (2016) 5933.

[15] Y. Liwei, G. Xiaoqing, L. Zhenchao & J. Dongyu, "Quantitative effects of air pollution on regional daily global and diffuse solar radiation under clear sky conditions", Energy Reports **8** (2022) 1935.

[16] P. Kyriakoula, F. Ilias, G. Antonis, K. G. Panagiotis, N. T. Panagiotis, Ha. Maria & K. Stelios, "15-Year Analysis of Direct Effects of Total and Dust Aerosols in Solar Radiation/Energy over the Mediterranean Basin", Remote Sensing **14** (2022) 1535.

[17] Y. A. Douanla, A. Dembélé, O. Mamadou & A. Lenouo, "Prediction of daily direct solar energy based on XGBoost in Cameroon and key parameter impacts analysis", 2022 IEEE Multi-conference on Natural and Engineering Sciences for Sahel's Sustainable Development (MNE3SD) (2022) 1.

[18] Y. A. Douanla, A. Dembélé, O. Mamadou, D. R. R. Koukoui, F. E. Akpoly & A. Lenouo, "Wavelet Analysis of the Interconnection between Atmospheric Aerosol Types and Direct Irradiation over Cameroon", Advances in Meteorology (2022).

[19] P. B. Donald & W. T. Andrew, *Wavelet methods for time series analysis*, Cambridge university press **4** (2000).

[20] S. Jevrejeva, JC. Moore & A. Grinsted, "Influence of the Arctic Oscillation and El Niño-Southern Oscillation (ENSO) on ice conditions in the Baltic Sea: The wavelet approach", Journal of Geophysical Research: Atmospheres, **108** (2003) D21.

[21] C. Pimwadee, G. Aryya, K. George & C. Zhiyuan, "Discrete wavelet transform-based time series analysis and mining", ACM Computing Surveys (CSUR) **43** (2011) 1.

[22] T. B. Godfrey, "Cameroon 55", Handbook of Global Bioethics, (2014) 941.

[23] P. Tchawa, "Le Cameroun: une Afrique en miniature?", Les Cahiers d'Outre-Mer. Revue de géographie de Bordeaux **65** (2012) 319.

[24] G. Aslak, J. C. Moore & S. Jevrejeva, "Application of the cross wavelet transform and wavelet coherence to geophysical time series", Nonlinear processes in geophysics **11** (2004) 561.

[25] K. Ladislav, "What are the main drivers of the Bitcoin price? Evidence from wavelet coherence analysis", PloS one **10** (2015) e0123923.

[26] J. Bitton *et al.*, *écosystème forestier et l'atmosphère au moyen de la transformée en ondelettes continue*, Université de Liège, Liège, Belgique (2019).

[27] E. KW . Ng & J. CL. Chan, "Geophysical applications of partial wavelet coherence and multiple wavelet coherence", Journal of Atmospheric and Oceanic Technology **29** (2012) 1845.

[28] C. Lara, B. Cazelles, G. S. Saldías, R. P. Flores, Á. L. Paredes & B. R. Broitman, "Coupled biospheric synchrony of the coastal temperate ecosystem in Northern Patagonia: a remote sensing analysis", Remote Sensing **11** (2019) 2092.

[29] C. Torrence & G. P. Compo, "A practical guide to wavelet analysis", Bulletin of the American Meteorological society **79** (1998) 1.

[30] H. Wei, *Matlab code for multiple wavelet coherence and partial wavelet coherency*, https://figshare.com/articles/software/Matlab_code_for_multiple_wavelet_coherence_and_partial_wavelet_coherency/13031123/2, (2020).

[31] H. Wei & S. Bing, "Improved partial wavelet coherency for understanding scale-specific and localized bivariate relationships in geosciences", Hydrology and Earth System Sciences **25** (2021).

[32] C. McSweeney, M. New & G. Lizcano, *UNDP climate change country profiles: Cameroon* (2008), https://www.geog.ox.ac.uk/research/climate/projects/undp-cp/UNDP_reports/Cameroon/Cameroon.hires.report.pdf, Oxford: United Nations Development Programme and University of Oxford.

[33] K. Matsuda, S. Nakae & K. Miura, "Origin and characteristics of sulfate aerosols in Tokyo", Journal of Japan Society for Atmospheric Environment/Taiki Kankyo Gakkaishi **33** (1998) 4.
[34] C. Liousse *et al.*, "Real time black carbon measurements in West and Central Africa urban sites", Atmospheric Environment **54** (2012) 529.
[35] P. PXiaole, Y. Kanaya & Z. Wang, "Correlation of black carbon aerosol and carbon monoxide in the high-altitude environment of Mt. Huang in eastern China", AGU Fall Meeting Abstracts (2011) A21B–0034.
[36] D. Fonkem *et al.* "Effects of season on the microbiological quality of Kilishi, a traditional Cameroonian dried beef product", Tropicultura **28** (2010) 10.